Influence of anions on the structure and morphology of steel rust particles prepared by aerial oxidation of acidic Fe(II) solutions

Hidekazu Tanaka,[a*] Nagisa Hatanaka,[a] Miya Muguruma,[a] Ayaka Nishitani,[a] Tatsuo Ishikawa[b], Takenori Nakayama[c]

[a] Department of Chemistry, Graduate School of Science and Engineering,
Shimane University,
1060 Nishikawatsu, Matsue, Shimane 690-8504, Japan

[b] School of Chemistry,
Osaka University of Education,
4-698-1 Asahigaoka, Kashiwara, Osaka 582-8582, Japan

[c] Materials Research Laboratory,
Kobe Steel, LTD.,
5-5 Takatsukadai 1, Nishi-ku, Kobe, Hyogo 651-2271, Japan

* responsible author
The name and address of the responsible author;
Prof. Hidekazu Tanaka
Department of Chemistry, Graduate School of Science and Engineering
Shimane University
1060 Nishikawatsu, Matsue, Shimane 690-8504
Japan
E-mail: hidekazu@riko.shimane-u.ac.jp
FAX: +81-852-32-6823

Abstract

In order to simulate the atmospheric corrosion of steel, artificial steel rust particles were synthesized by aerial oxidation of aqueous solutions containing $FeCl_2$, $FeSO_4$ and $NaNO_3$, and the structure and morphology of the obtained particles were characterized by XRD and TEM. Needle-like SO_4^{2-} containing Schwertmannite ($Fe_8O_8(OH)_6(SO_4)$) particles were mainly formed in $FeCl_2$−$FeSO_4$, $FeSO_4$−$NaNO_3$, $FeCl_2$−$FeSO_4$−$NaNO_3$ systems, and the crystallization and particle growth of this material were not influenced by added Cl^- and NO_3^-. The rod-shaped β-FeOOH particles were formed from in only $FeCl_3$-$NaNO_3$ system, though no marked change in crystallite and particle sizes of the β-FeOOH was recognized by adding NO_3^-. Accordingly, it can be suggested that the corrosive SO_X gas and air-borne chloride strongly affect the rust formation in atmospheric corrosion of the steels.

Keywords: Artificial steel rust, Atmospheric corrosion, Corrosive gas, Anion, Rust formation

1. Introduction

The formation and structure of atmospheric corrosion products of steels strongly depend on the exposure environment of steels [1-3]. The air-borne chloride, SO_X and NO_X in atmosphere are dissolved in thin film water on the steels to generate anions such as Cl^-, SO_4^{2-} and NO_3^-, respectively. Then, Fe^{2+} is eluted from the steels and a part of Fe^{2+} is oxidized to Fe^{3+} by dissolved O_2. Therefore, the rust formation on the steel can regard as the reaction of Fe^{2+}, Fe^{3+} and anions in water. As a result, the α-FeOOH, γ-FeOOH and Fe_3O_4 rusts are mainly generated in atmosphere including NO_X and SO_X such as urban and industrial zones, while the β-FeOOH rust is formed in Cl^--containing environment such as marine zone including air-borne chloride [1-3]. Nevertheless, the detail role of anions on the formation of steel rusts is not fully established. To clarify this, several researchers have studied of this subject [4-8]. Ishikawa et al. and Kamimura et al. reported that the formation of β-FeOOH rust particles is suppressed by added SO_4^{2-}, while no significant effect of NO_3^- is seen. [4,5] Also, Sudakar et al. reported that the solubility of γ-FeOOH particles is increased by adding Cl^- and SO_4^{2-} [6]. Further, Oh et al. synthesized the steel rust particles from a mixture of $FeSO_4$ and $FeCl_2$ solutions and indicated that the existence of SO_4^{2-} enhances the α-FeOOH formation [7]. On the other hand, the authors studied the influence of Cl^-, SO_4^{2-} and NO_3^- on the formation of steel rust particles prepared from acidic Fe^{3+} solutions and indicated that added Cl^- accelerates the β-FeOOH formation and addition of SO_4^{2-} markedly inhibits the rust formation [8]. However, these studies are mainly discussed on the steel rust particles synthesized from Fe^{3+} solutions except for the study by Oh et al [7]. In order to elucidate the atmospheric corrosion mechanism of steels at initial stage, systematic investigation about the influence of anions on the formation of steel rust particles prepared from Fe^{2+} solutions is more appropriate than that from Fe^{3+} solutions.

The purpose of this study was to clarify the influence of anions on the formation, structure and morphology of steel rust particles. So that, the artificial steel rust particles

are synthesized by aerial oxidation of a mixture of aqueous $FeCl_2$, $FeSO_4$ and $NaNO_3$ solutions. The products thus prepared were characterized by means of powder X-ray diffraction and transmission electron microscope. The obtained results must serve to elucidate the role of air-borne chloride, SO_X and NO_X on the rust formation in atmospheric corrosion of steels.

2. Experimental

2.1 Synthesis of steel rust particles

Artificial steel rust particles were prepared by aerial oxidation of acidic aqueous Fe^{2+} solutions in $FeCl_2$−$FeSO_4$, $FeCl_2$−$NaNO_3$, $FeSO_4$−$NaNO_3$ and $FeCl_2$−$FeSO_4$−$NaNO_3$ systems as follows. In $FeCl_2$−$FeSO_4$ system, 250 mL of a mixture of aqueous $FeCl_2$ and $FeSO_4$ solutions were prepared using deionized-distilled water. Then, the Fe^{2+} concentration was 1.0 mol/L and the molar ratio $X_{Cl} = FeCl_2/(FeCl_2 + FeSO_4)$ ranged from 0 to 1.0. In $FeCl_2$−$NaNO_3$, $FeSO_4$−$NaNO_3$ and $FeCl_2$−$FeSO_4$−$NaNO_3$ systems, desired amounts of $NaNO_3$ were added to 250 mL of 1.0 mol/L $FeCl_2$−$FeSO_4$ solution at molar ratio NO_3^-/Fe(II) = 0 − 1.0 and X_{Cl} = 0 − 1.0. Before the aging, pH of all the solutions was ca. 3.0. The solutions thus prepared were aged in a polypropylene vessel equipped with reflux condenser by aerial oxidation at 4 L/min and 50°C for 24 h. The formed precipitates were filtered off using 0.45 μm Millipore filter, thoroughly washed with distilled-deionized water and finally dried at 50°C for a over night. All the chemicals purchased from Wako Pure Chemical Industries Ltd., were used without further purification.

2.2 Characterization

The products thus formed were characterized by a variety of conventional techniques. Powder X-ray diffraction (XRD) patterns were taken on a Rigaku Miniflex-II diffractometer with a Ni-filtered CuKα radiation operated at 30 kV and 15 mA. The

scanning speed and step were 2°/min and 0.01°, respectively. Morphology of the obtained particles was observed by a TOPCON EM-002B transmission electron microscope (TEM) at 200 kV.

3. Results and Discussion

3.1 Yield of the products

Fig. 1 shows yield of the products in $FeCl_2$−$FeSO_4$, $FeCl_2$−$NaNO_3$, $FeSO_4$−$NaNO_3$, $FeCl_2$−$FeSO_4$−$NaNO_3$ systems. In $FeCl_2$−$FeSO_4$ system, yield of the products is 1.1 g at molar ratio $X_{Cl} = 0$ and is slightly decreased with the increase of X_{Cl}. In $FeSO_4$−$NaNO_3$ system, increasing NO_3^-/Fe(II) ratio faintly increases yield of the products. On the other hand, no remarkable change in yield of the products is seen in $FeCl_2$−$NaNO_3$ system. In case of $FeCl_2$−$FeSO_4$−$NaNO_3$ system, yield of the products is increased with the decrease of X_{Cl} and the increase of NO_3^-/Fe(II) ratio. These facts allow us to infer that adding SO_4^{2-} and NO_3^- accelerate the formation of steel rusts. The details of this will be discussed later.

3.2 Structure and morphology of rust particles formed in $FeCl_2$−$FeSO_4$, $FeSO_4$−$NaNO_3$ and $FeCl_2$−$NaNO_3$ systems

Fig. 2(A) shows the XRD patterns of the products formed in $FeCl_2$−$FeSO_4$ system at different X_{Cl}. At $X_{Cl} = 0 - 0.75$, the diffraction peaks characteristics of iron oxyhydroxysulfate named as Schwertmannite ($Fe_8O_8(OH)_6SO_4$) (PDF No. 47−1755) appear and the diffraction intensity is essentially unchanged by raising X_{Cl}. At $X_{Cl} = 1.0$, the Schwertmannite peaks disappear. Whereas, the β-FeOOH peaks (No. 34−1266) are developed in addition to Schwertmannite ones at $X_{Cl} = 0.75$ and are remarkably intensified at $X_{Cl} = 1.0$. The crystallite size of Schwertmannite estimated from the full width at half height of (212) peak using the Scherrer equation is almost constant of ca. 5 nm at $X_{Cl} = 0 - 0.75$. Fig. 2(B) displays the XRD patterns of the products yielded in

$FeSO_4$–$NaNO_3$ system at NO_3^-/Fe(II) = 0 − 1.0. At NO_3^-/Fe(II) = 0 − 0.75, the diffraction peaks due to Schwertmannite mainly develop and no remarkable change in diffraction intensity and crystallite size of this material is seen by increasing NO_3^-/Fe(II) ratio. Besides, new sharp peaks due to SO_4^{2-}-containing Natrojarosite ($NaFe_3(SO_4)_2(OH)_6$) (No. 51-1567) appear at NO_3^-/Fe(II) ≥ 0.50. At NO_3^-/Fe(II) = 1.0, the intensity of Natrojarosite peaks is much larger than that of Schwertmannite ones, meaning that the major product turns to be Natrojarosite. Fig. 2(C) demonstrates the XRD patterns of the products formed in $FeCl_2$–$NaNO_3$ system at different NO_3^-/Fe(II) ratios. At NO_3^-/Fe(II) = 0, all the peaks can be assignable to the β-FeOOH and the crystallite size evaluated from (310) peak is 45 nm. The diffraction intensity and crystallite size of this material are almost not changed by increasing NO_3^-/Fe(II) ratio. Besides, the peaks related to secondary phase are not detected over the whole NO_3^-/Fe(II) range.

Fig. 3 shows the TEM pictures of the particles obtained in $FeCl_2$–$FeSO_4$ system at various X_{Cl}. At X_{Cl} = 0, the needle-like Schwertmannite particles with a size of ca. 200 nm in length and ca. 20 nm in width are found. No marked changes in size and shape of the Schwertmannite particles are recognized by raising X_{Cl}. Whereas, the rod-shaped β-FeOOH particles with a size of ca. 120 nm in length and ca. 25 nm in width slightly appear in addition to the Schwertmannite ones at X_{Cl} = 0.75. At X_{Cl} = 1.0, the size of the β-FeOOH particles increases to ca. 150 nm (length) and ca. 30 nm (width), while the Schwertmannite particles disappear. These facts allow us to infer that added SO_4^{2-} inhibits the growth of β-FeOOH particles, though the addition of Cl^- has no significant effect on the growth of Schwertmannite particles. Fig. 4 shows the TEM pictures of the products generated in $FeSO_4$–$NaNO_3$ system at different NO_3^-/Fe(II) ratios. At NO_3^-/Fe(II) = 0 − 0.75, the needle-like Schwertmannite particles with a size of ca. 200 nm in length and ca. 20 nm in width are observed and the morphology of the particles are almost unchanged by increasing the NO_3^-/Fe(II) ratio. Besides, the hexagonal

Natrojarosite particles are found at NO_3^-/Fe(II) ≥ 0.5 and the particle size is increased to ca. 4 μm at NO_3^-/Fe(II) ratio = 1.0. Fig. 5 shows the TEM pictures of the particles formed in $FeCl_2$−$NaNO_3$ system at various NO_3^-/Fe(II) ratios. At NO_3^-/Fe(II) = 0, the rod-shaped β-FeOOH particles with a size of ca. 150 nm in length and ca. 30 nm in width appear, though no remarkable change in morphology of β-FeOOH particles is recognized over the whole NO_3^-/Fe(II) range. It is, therefore, indicative that the growth of Schwertmannite and β-FeOOH particles is not influenced by added NO_3^-.

From these results, influence of anions on the formation of steel rust particles is in order of SO_4^{2-} > Cl^- >> NO_3^-. The addition of SO_4^{2-} and Cl^- respectively accelerates the formation of Schwertmannite and β-FeOOH particles, nonetheless the formation and growth of steel rust particles are essentially not affected by added NO_3^-.

3.3 Structure and morphology of rust particles formed in $FeCl_2$−$FeSO_4$−$NaNO_3$ system

Fig. 6 shows the XRD patterns of the products formed in $FeCl_2$−$FeSO_4$−$NaNO_3$ system at different X_{Cl} and NO_3^-/Fe(II) ratios. At X_{Cl} = 0.25 and NO_3^-/Fe(II) = 0.25 − 0.75, the major product is Schwertmannite, and the diffraction intensity and crystallite size of this material are almost constant. While, the major product turns to be Natrojarosite at NO_3^-/Fe(II) = 1.0. Similar tendency can be seen for the particles prepared at X_{Cl} = 0.50 and 0.75, although the intensity of Natrojarosite peaks is dramatically weakened by raising X_{Cl}. These facts reveal that added SO_4^{2-} remarkably accelerates the formation of SO_4^{2-}-containing Schwertmannite and Natrojarosite particles in $FeCl_2$−$FeSO_4$−$NaNO_3$ system, well in accordance with the results obtained in $FeCl_2$−$FeSO_4$ and $FeSO_4$−$NaNO_3$ systems.

Fig. 7 shows the TEM pictures of the particles generated in $FeCl_2$−$FeSO_4$−$NaNO_3$ system at various X_{Cl} and NO_3^-/Fe(II) ratios. At X_{Cl} = 0.25 and NO_3^-/Fe(II) = 0.25 − 0.75, the needle-like Schwertmannite particles with a size of ca. 200 nm in length and ca. 20 nm are formed and its particle morphology almost corresponds to that yielded at

NO_3^-/Fe(II) = 0. At NO_3^-/Fe(II) = 1.0, the hexagonal Natrojarosite particle with a size of ca. 5 μm is found. Similar tendency can be seen at X_{Cl} = 0.50 and 0.75, and the change in morphology of Schwertmannite particles by increasing NO_3^-/Fe(II) ratio is not recognized. These results mean that added Cl^- and NO_3^- do not affect the growth of Schwertmannite particles.

From the afore-mentioned results, we can summarize the major product in Fig. 8. The existence of SO_4^{2-} in $FeCl_2$−$FeSO_4$, $FeSO_4$−$NaNO_3$ and $FeCl_2$−$FeSO_4$−$NaNO_3$ systems forms the SO_4^{2-}-containing steel rust particles such as Schwertmannite and Natrojarosite. The β-FeOOH particles are mainly formed in $FeCl_2$−$NaNO_3$ system in the absence of SO_4^{2-}. While, the influence of NO_3^- on the structure and particle morphology of the steel rusts is negligibly small. These findings suppose that corrosive SO_X gas and air-born chloride affect the formation of steel rusts.

3.4 Influence of anions on the formation, structure and morphology of steel rust particles

It is well-known that hydrolysis and oxidation rates of Fe^{2+} are dependent of solution pH and the hydrolysis of Fe^{2+} takes place at pH ≥ 7 [9,10]. In the present study, pH of all the solution before aging is ca. 3, meaning the hydrolysis of Fe^{2+} to be difficult. It seems, therefore, that the steel rust particles are mainly formed from Fe^{3+} generated by aerial oxidation of Fe^{2+} in the solution via reaction (1).

$$Fe^{2+} + 1/2O_2 + H_2O \rightarrow Fe^{3+} + 2OH^- \qquad (1)$$

The formation of steel rusts in acidic Fe^{3+} solutions was reported as follows [11-14]. The hexa-aqua Fe^{3+} ions are produced by the reaction of Fe^{3+} with H_2O via reaction (2).

$$Fe^{3+} + 6H_2O \quad \square \quad [Fe(H_2O)_6]^{3+} \quad (2)$$

The $[Fe(OH)_n(H_2O)_{6-n}]^{3+}$ (n = 1 – 6) is generated by hydrolyzing the $[Fe(H_2O)_6]^{3+}$ via protolysis reaction (3).

$$[Fe(H_2O)_6]^{3+} + nOH^- \quad \square \quad [Fe(OH)_n(H_2O)_{6-n}]^{3+} + nH_2O \qquad (3)$$

The Fe−OH groups of the $[Fe(OH)_n(H_2O)_{6-n}]^{3+}$ respectively react with Fe−H_2O or Fe−OH groups of neighboring $[Fe(OH)_n(H_2O)_{6-n}]^{3+}$ via oxolation reaction (4) and olation reaction (5).

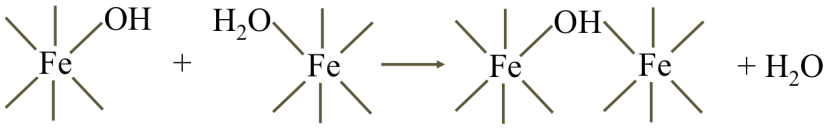

(4)

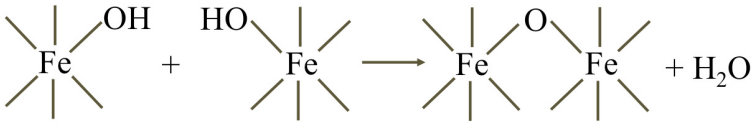

(5)

The reactions (1) – (5) continuously progress during aging under aerial oxidation to form various kinds of iron rust particles by passing through the nucleation and crystal growth processes. The addition of SO_4^{2-} would influence the formation of hexa-aqua Fe^{3+} ions. The stability constant (log *K*) of Fe^{3+}-complex with SO_4^{2-}, Cl^- and NO_3^- at 25°C are 4.1, 0.6 and 1.9, respectively, indicating that Fe^{3+} complex with SO_4^{2-} is much stable than that with Cl^- and NO_3^- [15]. It seems, therefore, that added SO_4^{2-} forms the SO_4^{2-}-containing aqua Fe^{3+} complexes via reaction (6).

$$Fe^{3+} + mSO_4^{2-} + (6-m)H_2O \rightarrow [Fe(SO_4)_m(H_2O)_{6-m}]^{3+} \quad (6)$$

Also, the $[Fe(OH)_n(SO_4)_m(H_2O)_{6-n-m}]^{3+}$ is formed from $[Fe(SO_4)_m(H_2O)_{6-m}]^{3+}$ via protolysis reaction (7).

$$[Fe(SO_4)_m(H_2O)_{6-m}]^{3+} + nOH^- \rightarrow [Fe(OH)_n(SO_4)_m(H_2O)_{6-n-m}]^{3+} + nH_2O \quad (7)$$

The protolysis, oxolation and olation reactions simultaneously and continuously proceed during aging to form SO_4^{2-}-containing Schwertmannite and/or Natrojarosite. On the other hand, $FeCl_2$−$NaNO_3$ system forms only β-FeOOH and no significant effect of added NO_3^- on the formation and growth of β-FeOOH particles is found. As has been already mentioned, the stability of Fe^{3+} complex with Cl^- and NO_3^- is much lower than that with SO_4^{2-}. Therefore, the reactions (1) - (5) are not suppressed by added Cl^- and NO_3^- during aging, resulting the formation of amorphous precursor of β-FeOOH particles. It has been reported that the zero point charge (*zpc*) of α-, β- and γ-FeOOH

particles is pH = 6 - 8 and these materials have a positive surface charge in acidic solutions [11]. Also, NO_3^- possesses a higher ionization energy than Cl^- [16]. Hence, added Cl^- preferentially adsorbed on the surface of amorphous precursor to crystallite as Cl^--containing β-FeOOH particles. As shown in Figs. 3 and 7, decreasing X_{Cl} reduces the size of β-FeOOH particles in $FeCl_2$−$FeSO_4$ and $FeCl_2$−$FeSO_4$−$NaNO_3$ systems, being indicative of the inhibition of growth of β-FeOOH particles by added SO_4^{2-}. This seems due to the adsorption of SO_4^{2-} on the surface of amorphous precursor of β-FeOOH particles. Whereas, as indicated in Fig. 1, yield of the products is increased with an increase of X_{Cl}. It has been reported that the solubility of β-FeOOH is larger than that of Schwertmannite because of the solubility product ($\log K_{sp}$) of Schwertmannite and β-FeOOH to be -40.0 and -39.0, respectively [11,17]. Accordingly, the increase of yield of the products is thought to be due to the formation of Schwertmannite with less solubility than β-FeOOH.

From the obtained results, adding SO_4^{2-} and Cl^- strongly affect on the formation, structure and morphology of artificial steel rust particles. These findings suggest that SO_X and air-borne chloride markedly influence the rust formation in atmospheric corrosion of steels.

4. Conclusions

In order to elucidate the influence of air-borne chloride and corrosive gasses such as SO_X and NO_X in atmosphere on the formation of steel rusts, artificial steel rust particles were prepared by aerial oxidation of a mixture of $FeCl_2$, $FeSO_4$ and $NaNO_3$ solutions and the structure and morphology of the obtained particles were examined. The summary of the present study can be drawn as follows.

(1) Adding SO_4^{2-} accelerates the formation of SO_4^{2-}-containing steel rust particles such as Schwertmannite and Natrojarosite, while there is no significant effect of Cl^- and NO_3^- on the formation of these rust particles.

(2) The β-FeOOH rust particles are mainly formed in $FeCl_2$−$NaNO_3$ system, whereas the influence of NO_3^- on the β-FeOOH formation is negligibly small.

(3) The formation of steel rust particles in acidic Fe^{2+} solution is dependent of the stability of Fe^{3+}-complexes with anions and the effect is in order of $SO_4^{2-} > Cl^- >> NO_3^-$.

(4) In atmospheric corrosion of steels, SO_X and air-borne chloride strongly affect the rust formation.

Acknowledgement

The authors grateful thank to Mr. Tsunao Yoneyama of Department of Biosignaling and Radioisotope Experiment Center for Integrated Research in Science of Shimane University for his help with TEM observation. This study was supported by JSPS KAKENHI Grant Number 23760699 and 26420739.

References

[1] J. D. Bernal, D. R. Dasgupta, A. L. Mackay, The oxides and hydroxides of iron and their structural inter-relationships, Clay Miner. Bull. 4 (1959) 15-30.

[2] P. Keller, Occurrence, formation and phase transformation of β-FeOOH in rust, Werkst. Korros. 20 (1969) 102-108.

[3] C. Leygraf, T. E. Graedel, Atmospheric Corrosion, Wiley-Interscience, New York, 2000.

[4] T. Ishikawa, S. Miyamoto, K. Kandori, T. Nakayama, Influence of anions on the formation of β-FeOOH rusts, Corros. Sci. 47 (2005) 2510-2520.

[5] T. Kamimura, S. Nasu, T. Segi, T. Tazaki, H. Miyuki, S. Morimoto, T. Kubo, Influence of cations and anions on the formation of β-FeOOH, Corros. Sci. 24 (2005) 2531-2542.

[6] S. Sudakar, G. N. Subbanna, T. R. N. Kutty, Effect of anions on the phase stability of γ-FeOOH nanoparticles and the magnetic properties of gamma-ferric oxide derived

from lepidocrocite, J. Phys. Chem. Solids 64 (2003) 2337-2349.

[7] S. J. Oh, S. J. Kwon, J. Y. Lee, J. Y. Yoo, W. Y. Choo, Oxidation of Fe^{2+} ions in sulfate- and chloride-containing aqueous medium, Corrosion 58 (2002) 498-504.

[8] H. Tanaka, N. Hatanaka, M. Muguruma, T. Ishikawa, T. Nakayama, Influence of anions on the formation of artificial steel rust particles prepared from acidic aqueous Fe(III) solution, Corros. Sci. 66 (2013) 136-141.

[9] B. Morgan, O. Lahav, The effect of pH on the kinetics of spontaneous Fe(II) oxidation by O_2 in aqueous solution--basic principles and a simple heuristic description, Chemosphere 68 (2007) 2080-2084.

[10] C. F. Baes, R. Mesmer, The Hydrolysis of Cations, Wiley, New York, 1976.

[11] R. M. Cornell, U. Schwartzmann, The Iron Oxides, VCS, Weinheim, 1996.

[12] T. Misawa, K. Hashimoto, S. Shimodaira, On the mechanism of atmospheric rusting of iron and protective rust layer on low alloy steels, Boshoku-Gijutsu 23 (1974) 17-27.

[13] M. Schultz, W. Burckhardt, S. T. Barth, Investigations on thermally forced hydrolysis and phase formation in aqueous iron(III) nitrate solutions, J. Mater. Sci. 34 (1999) 2217-2227.

[14] H. Tamura, The role of rusts in corrosion and corrosion protection of iron and steel, Corros. Sci. 50 (2008) 1872-1883.

[15] L. G. Sillen, A. E. Martell, Stability Constants of Metal-Ion Complexes, The Chemical Society, London, 1964.

[16] Chemical Handbook (Kagaku-Binran) 4th, Maruzen, The Chemical Society of Japan, Tokyo, 1993.

[17] J. Y. Yu, M. Park, J. Kim, Solubilities of synthetic schwertmannite and ferrihydrite, Geochem. J. 36 (2002) 119-132.

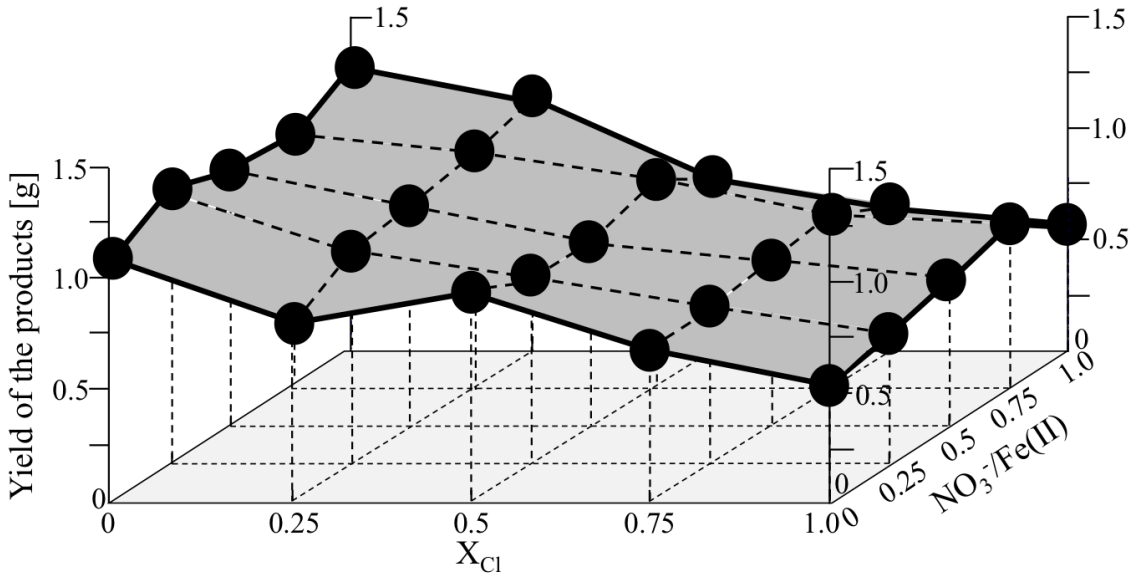

Fig. 1 Yield of the products formed in $FeCl_2$−$FeSO_4$−$NaNO_3$ system.

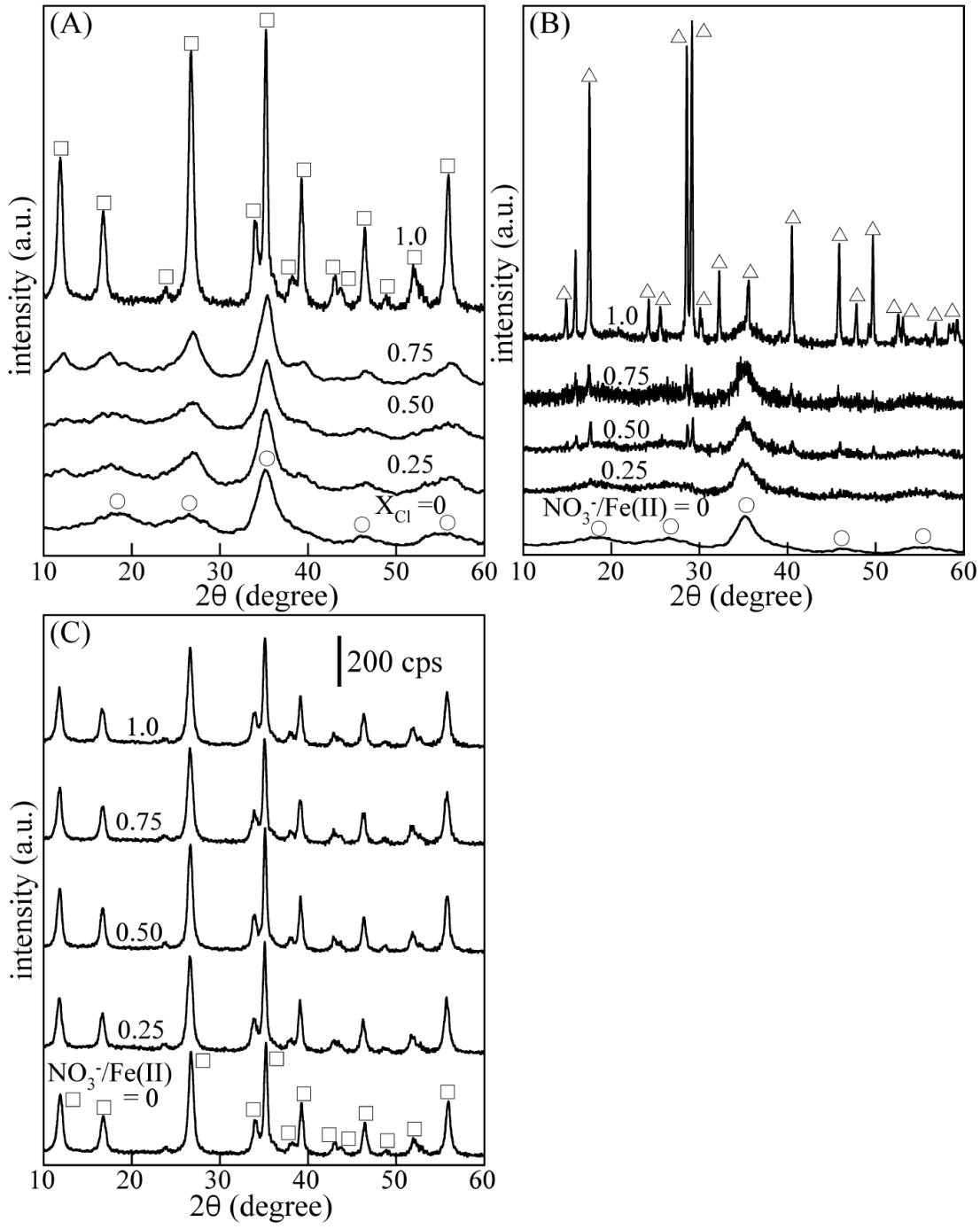

Fig. 2 XRD patterns of the products formed at different molar ratios X_{Cl} and NO_3^-/Fe(II) in (A) $FeCl_2$−$FeSO_4$, (B) $FeSO_4$−$NaNO_3$ and (C) $FeCl_2$−$NaNO_3$ systems. ○: Schwertmannite, △: Natrojarosite, □: β-FeOOH.

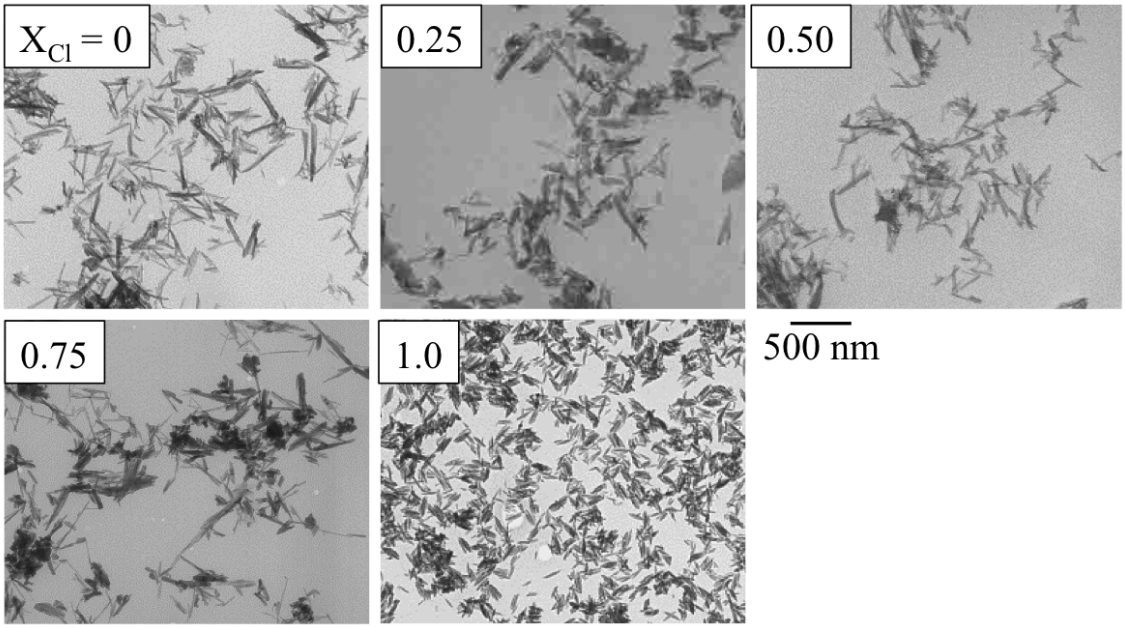

Fig. 3 TEM pictures of the particles yielded at different X_{Cl} in $FeCl_2$−$FeSO_4$ system.

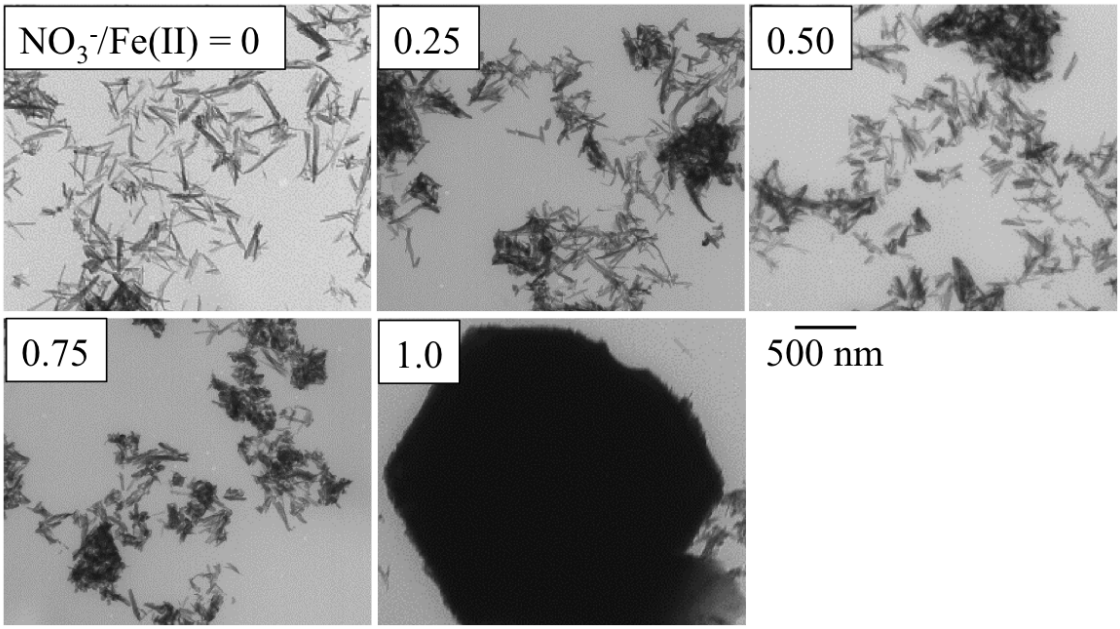

Fig. 4 TEM pictures of the particles formed at different NO_3^-/Fe(II) ratios in $FeSO_4$–$NaNO_3$ system.

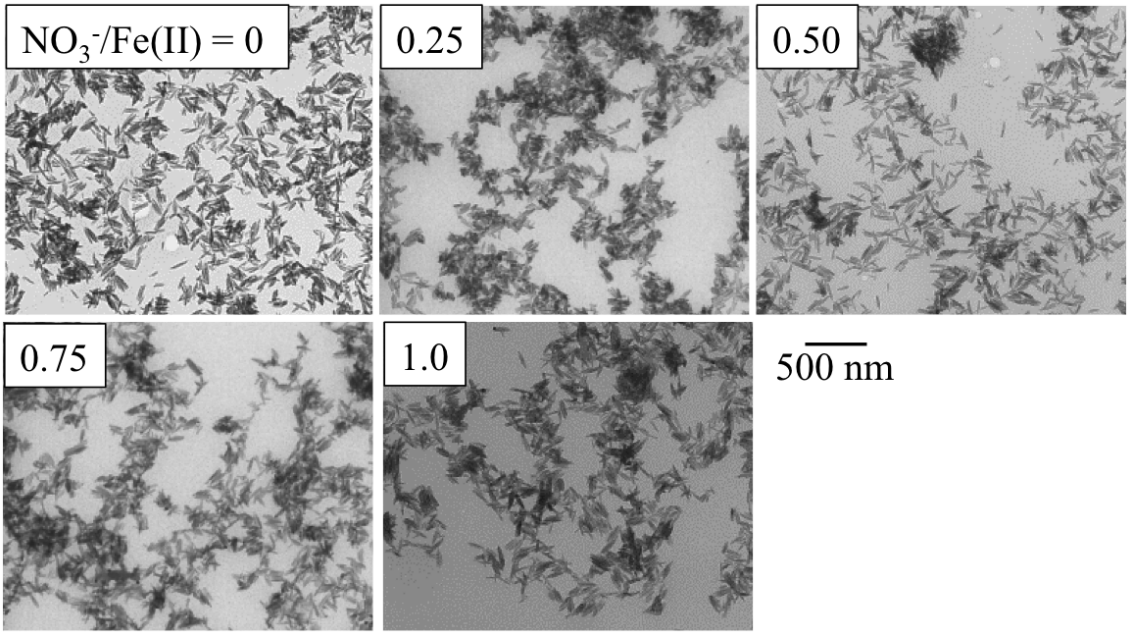

Fig. 5 TEM pictures of the particles generated at various NO_3^-/Fe(II) ratios in $FeCl_2$−$NaNO_3$ system.

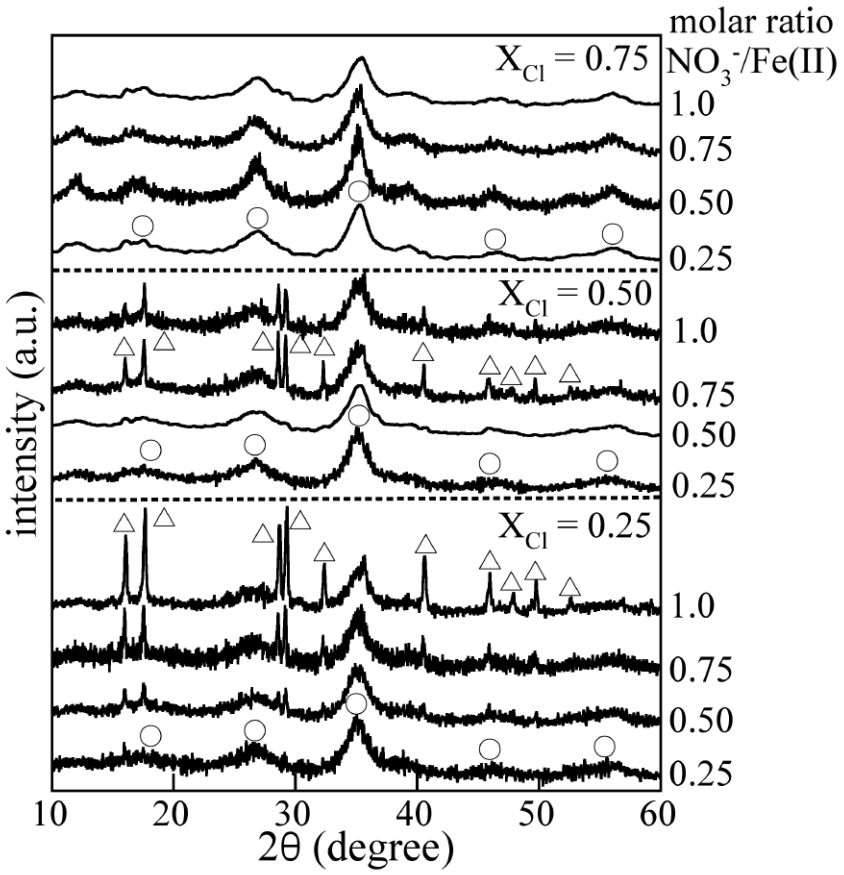

Fig. 6 XRD patterns of the products formed at different molar ratios X_{Cl} and NO_3^-/Fe(II) in $FeCl_2$−$FeSO_4$−$NaNO_3$ system. ○: Schwertmannite, △: Natrojarosite, □: β-FeOOH.

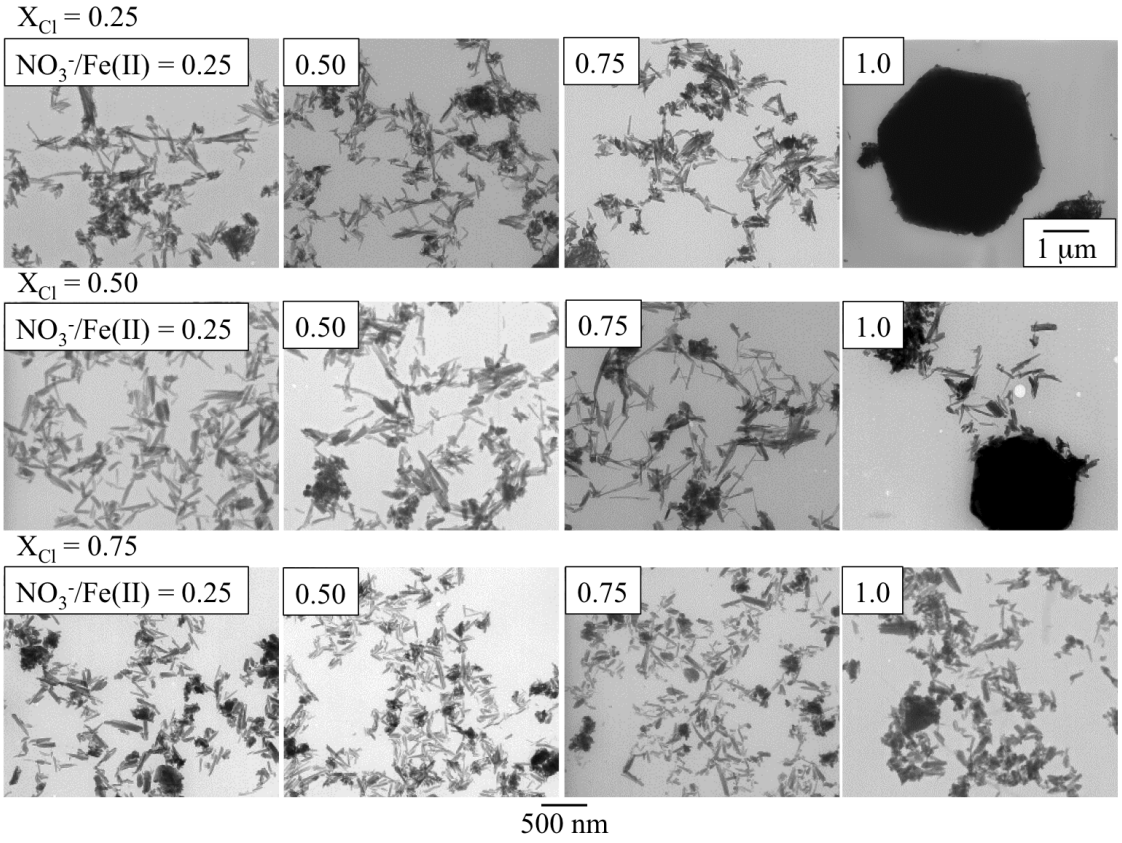

Fig. 7 TEM pictures of the particles yielded at various molar ratios X_{Cl} and NO_3^-/Fe(II) in $FeCl_2$−$FeSO_4$−$NaNO_3$ system.

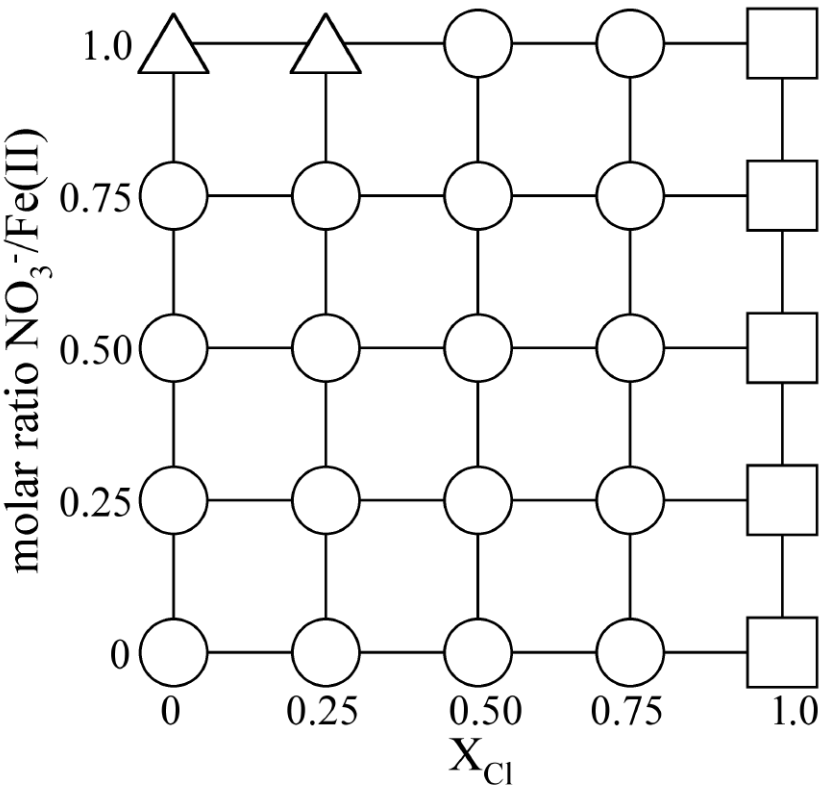

Fig. 8 Major product formed in $FeCl_2$−$FeSO_4$−$NaNO_3$ system. ○: Schwertmannite, △: Natrojarosite, □: β-FeOOH.